Physics – Uspekhi **69** (8) 774 – 784 (2026) ©2026 Uspekhi Fizicheskikh Nauk, Russian Academy of Sciences

REVIEWS OF TOPICAL PROBLEMS PACS numbers: 87.16.Ka, 87.16.Wd, 87.17.Ee

Microtubules are the simplest biomechanical engine that drives chromosome separation during cell division

I.V. Gonchar, G.S. Timoshin, N.B. Gudimchuk, F.I. Ataullakhanov

DOI: https://doi.org/10.3367/UFNe.2025.12.040069

Contents

1. Introduction **774**
2. Microtubule as a motor **775**
2.1 Structure and dynamics of microtubules; 2.2 Theoretical and experimental analysis of translocational capabilities of depolymerizing microtubules; 2.3 Mechanics of protofilament bending and its interaction with an attached bead; 2.4 The effect of counteracting load on the bending of a protofilament and the disassembly of a microtubule
3. 'Couplers' — molecular devices for coupling microtubule depolymerization with the processive motion of a load **779**
3.1 The first realistic coupler model — a 'Hill sleeve;' 3.2 Dam1 ring coupler; 3.3 Physical constraints on processive coupling by a Dam1-like ring; 3.4 Experimental analysis of Dam1-dependent coupling; 3.5 Fibrillar protein complexes as couplers in mammalian cells
4. Conclusion **783**
References **784**

Abstract. Humanity has invented many devices capable of performing diverse movements and mechanical work. All of these devices are macroscopic objects. Remarkably, however, every mechanical engine found in living nature is of molecular scale, no larger than 100 nm. Even to move an elephant or a whale, the Nature assembles complexes made of billions of such molecular motors instead of constructing a single large engine. We do not yet fully understand the advantages of this strategy, but one aspect is clear. Molecular motors utilize chemical energy to perform mechanical work, but they do not rely on elevated temperatures or pressures. Remarkably, the efficiency of these engines often greatly exceeds that of an internal combustion engine. Therefore, it is of great interest to understand how molecular motors function and how they have evolved. Among the most primitive molecular devices capable of moving molecular cargo are microtubules. Microtubules are ubiquitous cytoskeletal polymers that are critical for maintaining the cell's shape and structure, its viability, and its proper functioning. Besides their structural roles, microtubules enable the separation of chromosomes during cell division — a key process for all life. Microtubule dynamics involve a biochemical stage in which the high-energy molecule GTP is hydrolyzed, and the released energy becomes stored in the strained conformation of the microtubule. Only recently has it become fully clear that this stored conformational energy can be harnessed by the cell to perform the work of separating and transporting sister chromosomes to the opposite cellular poles during cell division. This appears to be some of the most ancient molecular mechanochemical engines operating within the cell.

Keywords: microtubule, force generation, mechanochemical engine, optical trap, cell division

I.V. Gonchar [1, a], **G.S. Timoshin** [1, b], **N.B. Gudimchuk** [1, 2, c], **F.I. Ataullakhanov** [1, 3, d]
[1] Center for Theoretical Problems of Physicochemical Pharmacology RAS, ul. Srednyaya Kalitnikovskaya 30, 109029 Moscow, Russian Federation
[2] Lomonosov Moscow State University, Faculty of Physics, Leninskie gory 1, str. 2, 119991 Moscow, Russian Federation
[3] Moscow Institute of Physics and Technology (National Research University), Institutskii per. 9, 141701 Dolgoprudny, Moscow region, Russian Federation
E-mail: [a] gonchar94@gmail.com, [b] timoshin.gs19@physics.msu.ru, [c] ngudimch@gmail.com, [d] ataullakhanov.fazly@gmail.com

Received 3 November 2025
Uspekhi Fizicheskikh Nauk **196** (8) 829 – 841 (2026)
Translated by the authors

1. Introduction

Living cells exist far from thermodynamic equilibrium, continuously consuming energy to maintain the internal organization of their contents, generate forces, and carry out directed processes in an environment in which thermal fluctuations occur continuously. Many key cellular functions are implemented using biomechanical devices at the level of individual molecules and their complexes, which, in a broad sense, are called molecular machines [1]. One type of such machines are linear motor proteins. These include kinesins and dyneins, which move along microtubules — the main structural elements of the cytoskeleton [2, 3]; myosins, which move along the more flexible elements of the cytoskeleton — actin filaments [4]; as well as nucleic acid motors — helicases and translocases — which move directionally along DNA or RNA [5, 6]. Linear motor proteins perform a wide variety of functions: for instance, they enable intracellular transport,

mediate cell division, drive the movement of cilia and flagella, mediate muscle contraction, participate in changes in cell shape, and perform mechanical work to unwind, separate, or reorganize nucleic acids and nucleoprotein complexes during processes such as replication, transcription, and repair, as well as in RNA-dependent stages of gene expression [5, 7, 8]. Another type of motor proteins are rotary molecular motors, primarily F_1F_0-synthases, which generate torque by linking ion gradients across membranes to ATP synthesis or hydrolysis. Related to them are ATP-dependent ion pumps that facilitate ion transport and acidification of organelles, as well as motors that drive bacterial flagella [9]. All of the listed types of molecular machines cyclically consume energy, most often in the form of energy released during the hydrolysis of an ATP molecule, or by using the energy of transmembrane ion gradients, converting this energy into useful mechanical work.

Compared to linear and rotational motors, microtubules are rather unusual biomechanical motors: they are dynamically unstable biopolymers that spontaneously switch between phase states [10]. Unlike linear and rotational motors, which operate in much the same way as macroscopic motors created by humans, microtubules function as active tracks for transport. They not only enable linear motors (such as kinesins and dyneins) to move loads along them, but they themselves constantly polymerize and depolymerize generating forces at their ends. These molecular devices have no obvious human-made counterparts, yet they are the basic and vital motors in cells, the Nature has precisely assigned them a key role in cell division that constitutes the most fundamental process of life reproduction. This paper focuses on one specific class of processes dependent on microtubules — particularly those that enable the development of mechanical forces and the performance of work by utilizing the energy from microtubule depolymerization.

2. Microtubule as a motor

Microtubules participate in a variety of cell's tasks throughout its lifetime: they are one of the main structural elements of the cell [11, 12]; they provide transport highways ('rails') for the movement of motor proteins within the cell; they are the main component of various cilia and flagella used by the cell for movement; finally, they themselves act as motors that ensure directed mechanical movement of chromosomes during cell division. In this chapter, we examine the main structural and dynamic properties of microtubules that enable them to perform this last and perhaps most important task — cell division.

2.1 Structure and dynamics of microtubules

The microtubule wall comprises tubulin dimers organized into a spiral structure, typically consisting of 13 linear chains of longitudinally linked tubulin dimers, known as protofilaments (Fig. 1). In this arrangement, each tubulin subunit contacts four neighbours: two lateral and two longitudinal. Only the tubulin subunits at the ends of the microtubule, where new tubulin dimers can attach from the solution, have fewer contacts. In the cytoplasm, the concentration of tubulin dimers reaches 24 μM [13]. The dynamics of microtubules depend on several small molecules that participate in the cell's energy metabolism: guanosine triphosphate (GTP) and guanosine diphosphate (GDP), whose concentrations in the cytoplasm are 100–200 μM and 10–20 μM, respectively [14],

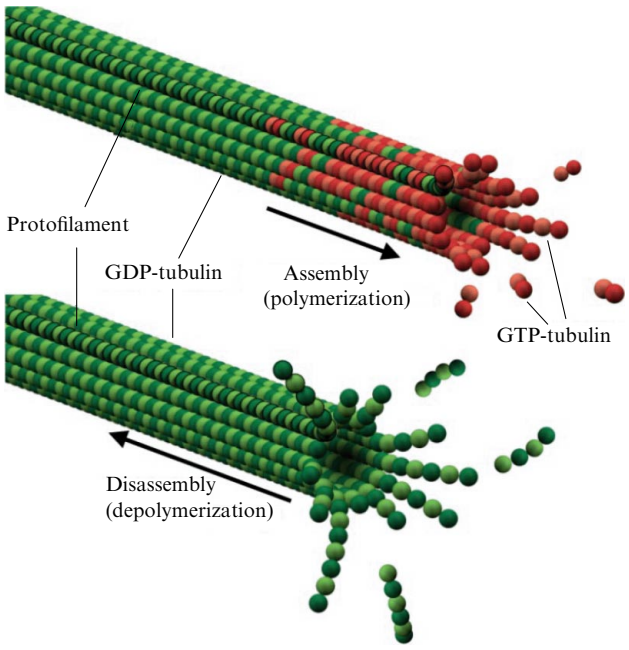

Figure 1. Structure and dynamics of a microtubule.

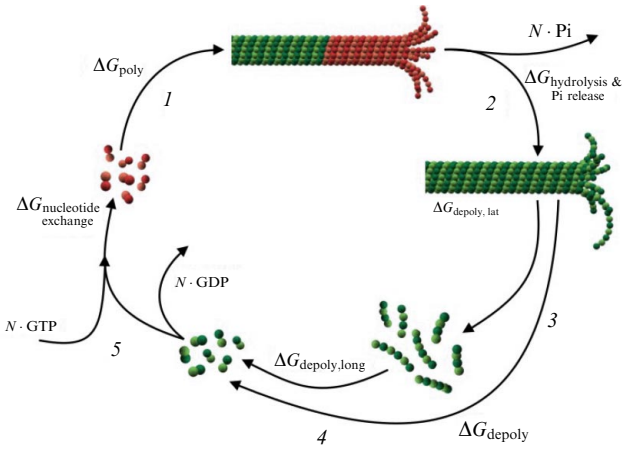

Figure 2. The thermodynamic cycle of microtubule polymerization and depolymerization (adaptation from [16, 17]). The numbers near arrows correspond to the stages of the thermodynamic cycle outlined in the text.

as well as magnesium ions and phosphate, whose concentrations are approximately 15–25 mM and 1 mM, respectively [14, 15]. All tubulin dimers are capable of binding and cleaving a GTP molecule. In the cytoplasm, most free tubulin dimers are bound to GTP molecules and magnesium ions. The polymerization and depolymerization of tubulin are associated with the reaction of turning a GTP molecule into GDP. In other words, these processes are associated with the consumption of the chemical energy stored in the GTP molecule.

Figure 2 shows the polymerization-depolymerization cycle of a microtubule. The main stages of this cycle are (*1*) polymerization of a microtubule from GTP-tubulins; (*2*) hydrolysis of GTP in the microtubule lattice, followed by the release of phosphate; (*3*) depolymerization of the GDP microtubule lattice into GDP-tubulin oligomers; (*4*) longitudinal rupture of GDP-tubulin oligomers; and finally, (*5*) nucleotide exchange, i.e., the release of GDP molecules and the binding of GTP molecules to tubulin dimers. It is

obvious that microtubule dynamics consumes energy: as a result of the cycle, N GTP molecules are converted into N GDP molecules and N inorganic phosphates.

When GTP-tubulins are incorporated into the microtubule wall, the rate of hydrolysis of GTP bound to tubulin increases by two orders of magnitude, since the longitudinally attached tubulin dimers lower the barrier for this reaction [18, 19]. Thus, most tubulin-associated GTP molecules are hydrolyzed shortly after their incorporation into the microtubule [20]. Therefore, most of the tubulin in the microtubule wall is GDP-tubulin. However, when GDP occupies the β-tubulin site of soluble tubulin dimers, the protein does not polymerize [21]. It is believed that this situation explains the fact that microtubules can undergo 'catastrophes,' in which slow polymerization suddenly turns into rapid depolymerization. This behavior is referred to as 'dynamic instability' [22].

Structural studies suggest that a tubulin dimer with GDP bound to its β-subunit is curved, so it does not fit neatly into the microtubule wall [23]. Thus, polymerized GDP-tubulin apparently cannot adopt its normal conformation due to the bonds formed with neighboring subunits in adjacent protofilaments. When a microtubule depolymerizes, these bonds dissociate, and the shortened end of the microtubule appears in a zone of laterally unbound protofilaments, which bend by approximately 22° with each tubulin dimer in the chain [24]. This shape is usually interpreted as reflecting the minimum energy form of GDP-tubulin dimers. Thus, the protofilament in the microtubule wall is a linear structure made up of GDP-tubulin dimers that tend to bend. The growing region of the microtubule, containing newly assembled tubulins whose GTP molecules have not yet undergone hydrolysis, forms a stabilizing cap (see Fig. 1) [20, 25]. This 'GTP cap' protects the microtubule from the transition from assembly to disassembly [26].

Although there is a great body of evidence confirming the existence of the GTP cap, its size and stabilization mechanism remain debatable [12, 27]. Thanks to this cap, a microtubule can incorporate many hundreds of new GTP-tubulin molecules, thereby elongating by tens of micrometers. When, by chance, the GTP cap structure contains a fairly large number of tubulin molecules that have managed to transition to the GDP state due to the stochastic nature of the GTP hydrolysis process, or when the cap weakens due to asynchronous elongation of the protofilaments [28 – 30], a transition to shortening occurs, known as a catastrophe [31]. Depolymerization proceeds differently than polymerization. Instead of step-by-step detachment of individual GDP-tubulin molecules, lateral bonds are cleaved first. Then individual protofilaments detach from each other, and only after that do the longitudinal bonds begin to rupture. The sequential rupture of bonds greatly facilitates the depolymerization process, which is why the microtubule depolymerizes at rates an order of magnitude higher than the polymerization rate. The protofilaments released from the microtubule body tend to adopt bent configuration at equilibrium. During this bending, they can perform mechanical work.

The following estimate of the maximum energy that a microtubule can use to perform mechanical work during depolymerization can be made. The change in free energy of the system, equal to the energy of N GTP molecules hydrolysis, is distributed among the stages of the cycle as follows [16]:

$$\Delta G_{\mathrm{GTP}} = \Delta G_{\mathrm{poly}} + \Delta G_{\mathrm{hydrolysis,\,Pi\ release}} + \Delta G_{\mathrm{depoly}} + \Delta G_{\mathrm{nucl.\ exchange}}\,, \quad (1)$$

where ΔG_{poly} is the energy of GTP-tubulin polymerization, $\Delta G_{\mathrm{hydrolysis,\,Pi\ release}}$ is the energy of GTP hydrolysis and phosphate release from the lattice, $\Delta G_{\mathrm{depoly}}$ is the energy of GDP lattice depolymerization, and $\Delta G_{\mathrm{nucl.\ exchange}}$ is the GDP-GTP exchange energy in free tubulin dimers.

Equation (1) is written per one GTP molecule. This equation imposes important thermodynamic constraints on the magnitude of the forces that can be exerted during the growth and shortening of microtubules. The maximum force generated by microtubule depolymerization can be estimated assuming that all $\Delta G_{\mathrm{depoly}}$ energy is converted into mechanical work over a distance d:

$$F = -\frac{\Delta G_{\mathrm{depoly}}}{d}\,. \quad (2)$$

The energy of GDP lattice depolymerization, $\Delta G_{\mathrm{depoly}}$, can be estimated from Eqn (1) as described in [16]. Total energy of GTP hydrolysis in cells is roughly -12.5 kcal mol^{-1}; $\Delta G_{\mathrm{poly}} = RT\ln(c/c_{\mathrm{cr}}) = -3$ kcal mol^{-1}; the free energy of nucleotides exchange $\Delta G_{\mathrm{nucl.\ exchange}} = -2$ kcal mol^{-1}; the free energy of GTP hydrolysis and phosphate release from the lattice is estimated to be -2.5 kcal mol^{-1}. Therefore, $\Delta G_{\mathrm{depoly}}$ is about -5 kcal mol^{-1}. Corresponding force according to Eqn (2) is ~ 60 pN per microtubule which is pretty impressive in the micro-world: this force drastically exceeds the force needed to move a mammalian chromosome through cytoplasm. Moreover, this value can explain a fascinating phenomenon: such chromosome motion was not hindered in experiments with chromosomes under loads of hundreds of piconewtons [32].

2.2 Theoretical and experimental analysis of translocational capabilities of depolymerizing microtubules

In 2005, precision experiments on individual microtubules provided the first direct evidence that depolymerization of microtubules generates forces that are significant by cellular standards [33]. In these experiments, a flow chamber was constructed on the surface of a cover glass. Seeds for microtubule growth were attached to the glass. When a tubulin solution was introduced into the chamber, artificial microtubules grew from the seeds. Roughly 10% of biotinilated (covalently modified with biotin) tubulin was added to the solution before its introduction into the chamber. After the microtubules grew to a length of approximately 10 μm, the tubulin solution was replaced with another solution in which rhodamine-labeled tubulin was associated with GMPCPP — a slowly hydrolyzable analogue of GTP. Thus, a stabilizing region grew at the end of the microtubule blocking disassembly (Fig. 3). A micron-sized bead coated with streptavidin was brought to the surface of the microtubule part, which was not stabilized by GMPCPP, using an optical tweezer. Streptavidin and biotin are known to form a highly stable biotin–streptavidin bond. Then the microtubule with the bead was positioned so that the bead would fit into the center of a laser trap calibrated to measure force.

After that, the chamber was illuminated with intense light in the rhodamine absorption band. This caused photodestruction of the stabilized end of the microtubule, and it began to disassemble [34]. The bead attached to the surface of the microtubule remained stationary until the depolymerization of the microtubule was triggered. As the microtubule depolymerized, the bead often exhibited a slight movement (jerk) in the direction of depolymerization before the bead

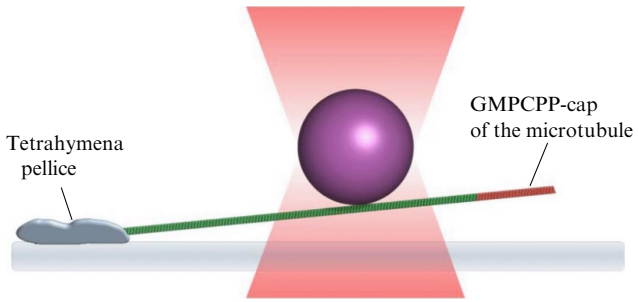

Figure 3. Depiction of the experiment to measure forces developed by a depolymerizing microtubule [33]. Initially, the bead is attached laterally to GDP-containing tubulins in the microtubule wall (green segment). Depolymerization of the microtubule is induced by photodestruction of the rhodamine-labeled GMPCPP-containing end of the microtubule (red segment). The cell membrane of the flagellated organism *Tetrahymena* was used as a source of seeds for microtubule nucleation.

became freely moving within the trap, since the part of the microtubule to which the bead was attached depolymerized.

Since this experimental system did not contain soluble proteins associated with the beads or soluble nucleotides, the jerk before the bead detachment must have been caused by conformational changes occurring at the shortening end of the microtubule when the depolymerization wave passed by the bead (Fig. 4a) [33]. The 'single' force jump recorded by the laser trap was small, barely reaching 0.5 pN. However, using a molecular-mechanical model of the microtubule, the authors came to the counterintuitive conclusion that this measured force amplitude corresponded to the action of a very efficient and powerful motor dependent on depolymerization.

2.3 Mechanics of protofilament bending and its interaction with an attached bead

To describe the behavior of this experimental system, the authors of [33] used a mathematical model of a microtubule, which provided the following interpretation of the experimental signals.

Taking into account the force acting on the bead at the center of a stationary optical trap (for details, see [35]), the evolution of the position of the bead is described by the Langevin equation in its general form:

$$m\frac{\mathrm{d}^2\mathbf{r}}{\mathrm{d}t^2}+\gamma\frac{\mathrm{d}\mathbf{r}}{\mathrm{d}t}=-\frac{\mathrm{d}U}{\mathrm{d}\mathbf{r}}+F(t)\,, \tag{3}$$

where U is total potential energy of the system comprising a microtubule bound to a bead in the optical trap force field; m is the bead's mass; γ is its friction coefficient; and $\mathbf{r}$ is a bead displacement vector. Function $F(t)$ describes Brownian noise. Microtubule depolymerization is relatively slow (10–500 nm s^{-1}), thus, we can neglect all acceleration terms. For typical microtubule disassembly rates, the second term in

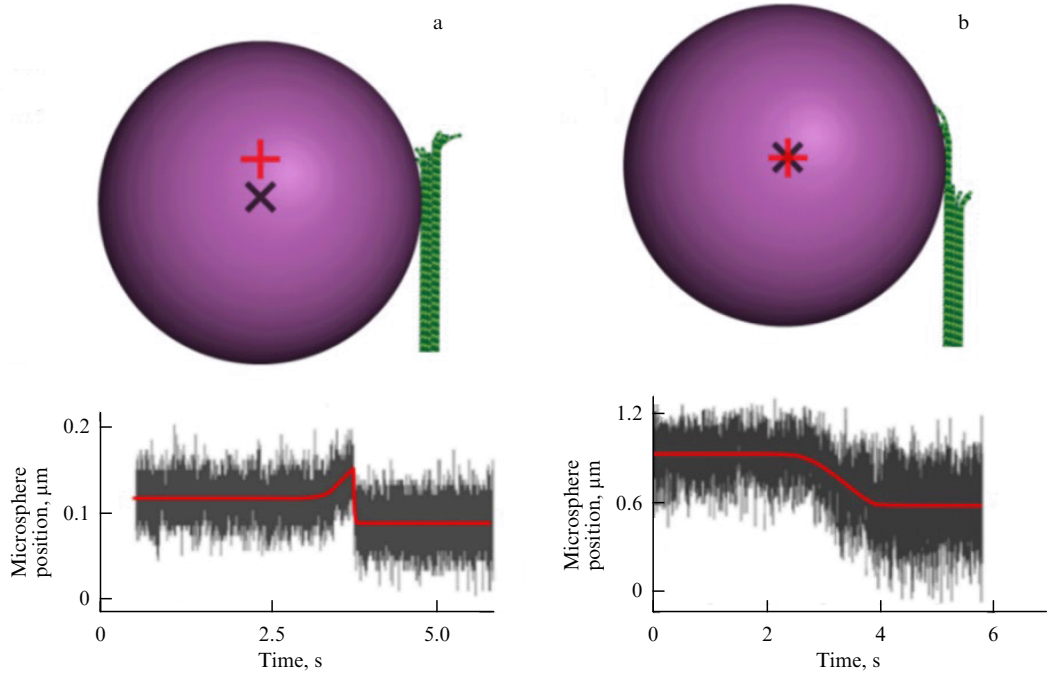

Figure 4. Scenarios for microtubule disassembly that lead to and did not lead to the development of force in experiments with a laser trap. (a) The plot shows the experimental signal recorded with a quadrant photodetector from a streptavidin-coated bead and a depolymerizing biotinylated microtubule. The bead's position oscillates rapidly (black curve) due to thermal noise (red line represents mean position). The cartoon above the signal illustrates the interpretation of the signal. Initially, the bead (not to scale) is attached to the stable wall of the microtubule and is influenced by a small force deliberately applied to straighten the configuration of the microtubule with the bead. Therefore, the center of the bead (black cross) is offset from the center of the trap (red cross). At the end of the experiment, the microtubule depolymerizes and the bead separates from it. Free from the microtubule but still captured by the trap, the bead exhibits a slightly greater average noise amplitude while located at the center of the trap. The transition between these states involves a rapid jump: the bead moves away from the center of the trap under the influence of the bending force of the protofilaments. Then, the tubulins associated with the bead detach from the end of the microtubule, and the bead abruptly falls into the center of the trap. (b) An example of an experimental signal demonstrating the flexibility of the protofilament tips. Under the forces from the trap, the protofilaments can bend in a direction opposite to that determined by their natural curvature. As a result, the microtubule cannot deflect the center of the ball from the center of the trap (the black and red crosses coincide).

Eqn (3) is also three orders of magnitude smaller than the developed forces. Furthermore, for millisecond and longer processes $\langle F(t)\rangle = 0$. Therefore, the bead position is fully governed by the following equation:

$$\frac{dU}{d\mathbf{r}} = 0 \qquad (4)$$

i.e., by the balance of the applied forces.

Two geometric objects — a 1 μm diameter sphere and 25 nm-diameter cylinder — can, in fact, contact each other only at a single geometric point. In reality, the microtubule and the protein-coated bead have a larger contact area, considering the ability of the protein molecules on the bead surface to stretch while bound to the microtubule. Calculations show that even in this case, the streptavidin-coated bead can bind to no more than three to five tubulin dimers along the length of one or two adjacent protofilaments [33]. For simplicity, the authors examined the mechanics of this system, assuming that the bead is attached laterally to a single protofilament in the microtubule wall. The diameter of the bead (1000 nm) was much larger than the linear region where the bead attached (20–60 nm). When depolymerization began, the lateral bonds between adjacent protofilaments broke down, and tubulin dimers containing GTP began to bend toward their minimum energy configuration. The local curvature of a fully bent protofilament containing GTP is significantly greater than that of a sphere (the curvatures are defined as the reciprocals of the radii of the most suitable circles for these shapes). Thus, the surface of the bead prevented the attached protofilament from reaching its equilibrium configuration, and the force of the bending dimers, F_{PF}, pushed the bead in a direction primarily perpendicular to the microtubule axis (Fig. 5).

Since the bead is placed in the force field of a focused laser beam, it also experiences a restoring force from the trap, F_{trap}. The microtubule has inherent, albeit small, flexibility, so when the F_{trap} pulls the bead, it deforms the microtubule (Fig. 5). The protofilament attached to the bead also deforms under the action of the trap's capture force. The elastic forces arising as a result of these deformations, as well as the stretching of the biotin–streptavidin bonds between the protofilament and the bead attached to it, lead to the F_{MT} reaction.

In equilibrium, the vector sum of F_{MT} and F_{PF} forces acts primarily along the microtubule axis in the direction of the disassembling tip (F_{sum}; Fig. 5). Figure 6 illustrates the time-lapse of computed bead–microtubule configurations in this system [33].

It is clear that, since the bead is rigidly attached to the protofilament, it cannot move along its surface. Instead, the bead rotates slightly as the system moves toward its stable configuration (Fig. 6). Calculations have shown that balance is achieved with a very small displacement of the bead in a direction perpendicular to the microtubule axis (about 7 nm for a 5500-nm-long microtubule with a bead diameter of 1000 nm and trap stiffness of 0.01 pN nm^{-1}). The displacement of the bead along the microtubule axis is somewhat greater (50–60 nm for these parameter values) and is achieved when the F_{trap} and F_{sum} components, parallel to the microtubule axis, become equal to each other. The magnitude of the force measured in the experiment (the F_{trap} component parallel to the microtubule; Fig. 5) is significantly less than the F_{PF} force with which the protofilament pushes against the bead. This mechanical interpretation is supported by experimental observations showing that smaller-diameter beads

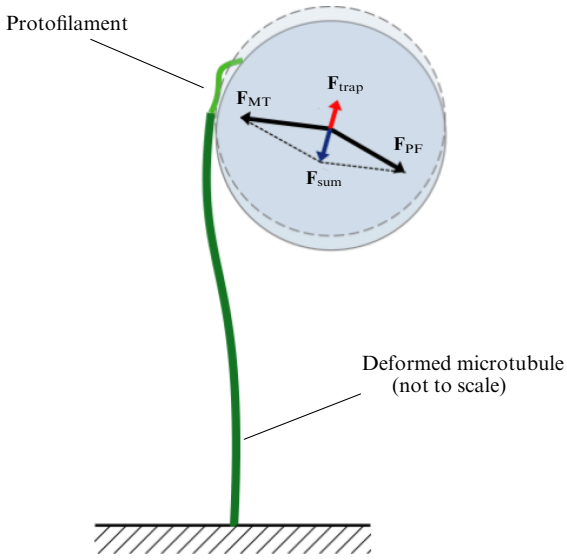

Figure 5. The forces acting on the bead attached to the protofilament. The initial position of the bead, attached to an intact microtubule, is shown by dashed lines. Subsequently, the bead moves (solid outline), pivoting around the point of attachment (see details in the text). The figure is adapted from [36].

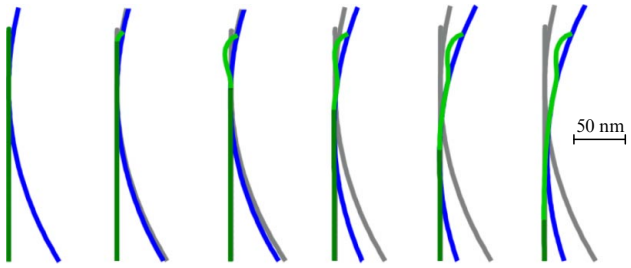

Figure 6. The computed configurations of the bead (blue line) and the depolymerizing microtubule (green line). When the microtubule begins to shorten, the tubulin subunits associated with the bead (light green) bend and slightly rotate the bead. The gray lines show the initial configuration of the system. The figure is adapted from [36].

yield greater recorded forces [37], consistent with this model's predictions (Fig. 7). Calculations have shown that a single protofilament, pressing on the attached bead with a force of about 5.8 pN, displaces a 1-μm-sized bead in the laser's force field by a distance corresponding to a trapping force of 0.5 pN. This value is in excellent agreement with the magnitude of the forces measured in experiments with streptavidin-coated beads (the maximum measured force was 0.45 pN) [33]. Therefore, if we account for the lever effect — where lever arm is essentially the radius of the bead — these experimental results imply that the force exerted by the bending protofilament in this experimental system is roughly 5.2 pN — only 1 pN less than the thermodynamic maximum [35].

It is appealing to compare the forces developed in this mechanical system with the forces acting on a 1-μm-diameter bead moving along a coverslip-attached microtubule via a kinesin motor protein. These systems share similar features: for instance, in both systems the bead is attached to the microtubule via protein bonds that have comparable characteristic size. Furthermore, as in the case of depolymerization-dependent motion, the kinesin-based system is relatively

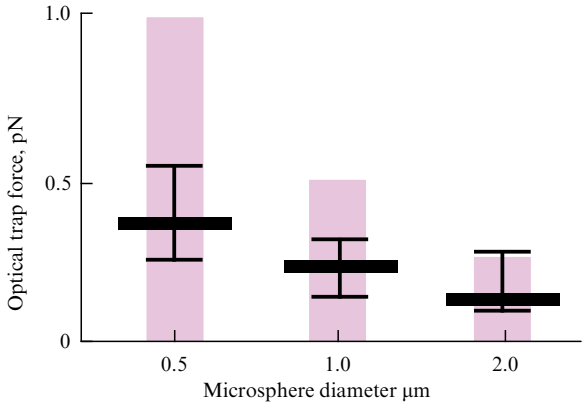

Figure 7. The force measured at the center of the bead depends on the bead's diameter. The horizontal lines correspond to the experimental signals (mean value with interquartile range) [37]. The purple bars represent the range of force amplitudes predicted by the model.

static, and the acceleration and viscous drag terms can be neglected. However, these systems have different geometric properties, since the kinesin moves along a microtubule that does not disassemble. When the kinesin starts moving, it applies a force to the surface of the bead in the direction of the motor's movement, while the trap capture force in the experiment with a depolymerizing microtubule is applied at the center of the bead. The force generated by the kinesin creates a torque that rotates the bead and pushes it against the wall of the microtubule. This force is counteracted by elastic forces from the wall. If the friction between the bead and the microtubule is negligible, a steady state is reached in which the kinesin-generated force is equal to the opposing force of the laser trap. When the protofilament bends, the geometry of the system is more complex and differs for different types of connections between the load and the end of the microtubule. To avoid misinterpretations, the relevant mechanics should be analyzed for each experimental system and type of attachment.

2.4 The effect of counteracting load on the bending of a protofilament and the disassembly of a microtubule

The analysis of the bead's movement kinetics under the depolymerization force, carried out in [33], provides additional details about the bead–microtubule interaction. Shortly after the microtubule depolymerization is initiated, the attached bead begins to move toward the stably attached minus-end of the microtubule, which moves the bead away from the center of the laser trap (see Fig. 4). This motion can be tracked with nanometer-level precision by measuring the bead's position using a quadrant photodetector.

The kinetics of changes in the bead coordinates should provide information about the rate at which the protofilaments attached to the bead generate force. If this interpretation is correct, the characteristic timescale of this movement should correspond to the rate of microtubule depolymerization. If this interpretation is correct, the characteristic time for this motion should correspond to the rate at which the microtubule disassembles. The rate of microtubule depolymerization depends on the Mg^{2+} concentration: at higher Mg^{2+} concentrations, microtubules disassemble faster. This prediction was tested using buffers with different concentrations of Mg^{2+} ions [38]. Indeed, the characteristic time for the rising phase of the force signal decreased with increasing Mg^{2+} concentration [33], as expected.

3. 'Couplers' — molecular devices for coupling microtubule depolymerization with the processive motion of a load

As described earlier, microtubule depolymerization plays a key role in one of the fundamental processes of life — chromosome segregation during cell division. Chromosomes in mitosis bind to the ends of microtubules via a specialized protein structure, the kinetochore. During cell division, chromosomes move along the ends of depolymerizing microtubules without losing contact with the depolymerizing end. Moreover, it is well known that in many cell types, microtubules shorten precisely at the end that is associated with the kinetochore [39]. The discovery that microtubule depolymerization can transport chromosomes, together with these features of chromosome motion, means that proteins associated with the kinetochore provide a stable connection between the chromosome and the shortening ends of the microtubules. These proteins can (1) efficiently use the energy of microtubule depolymerization to perform the work of processive chromosome motion and (2) ensure the stability of the attachment under high and variable loads. Thus, we come to the concept of a kinetochore 'coupler' — a macromolecular device that serves to couple the depolymerization process with the steady motion of the chromosome. Only the complete system including a depolymerizing microtubule together with a coupling device, or coupler, functions as a fully processive motor.

Let's focus on identifying the main features of theoretically possible and real couplers.

3.1 The first realistic coupler model — a 'Hill sleeve'

Terrell Leslie Hill would be famous for his outstanding contribution to theoretical biophysics even if he had not proposed the first explicit description of the kinetochore-microtubule coupling mechanism [40]. But this speculative mechanism, commonly referred to as the 'Hill sleeve,' had a significant impact on research in mitosis, and the corresponding 1985 publication is an essential citation in any review on this topic. This theoretical model, based on the classical idea of biased diffusion, was very influential, partly because it was both specific and quantitative. The term 'biased diffusion' refers to diffusive motion in which the system has a tendency to drift, moving with some preference in a certain direction. Hill [40] provided a detailed description of the 'sleeve' design — a cylindrical device that surrounds and interacts with the end of a microtubule (Fig. 8). He demonstrated that, given reasonable values for the model parameters, this sleeve can move together with the shortening end of the microtubule which became a fundamental discovery.

The sleeve proposed by Hill is a rigid, narrow tube located at the kinetochore that is only slightly wider than a microtubule and has a length of about 40 nm (Fig. 8a). Although the probability of a growing microtubule tip entering such a narrow channel might seem negligible, Hill calculated that this would not be an improbable event [40]. However, subsequent studies from other researchers demonstrated that capturing all 46 chromosomes (as in human cells) within a reasonable timeframe requires additional assumptions regarding microtubule-chromosome interactions [41]. But let's not dwell on this and assume that this is indeed feasible. A 40-nm-long channel corresponds approximately to the length of 5 tubulin dimers in one protofilament. In a microtubule consisting of 13 protofilaments, the sleeve can

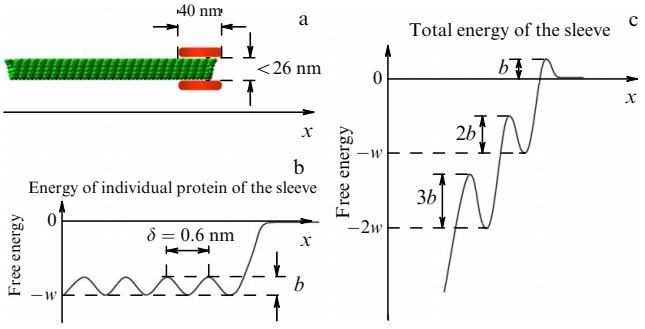

Figure 8. The energy of interactions in the 'Hill sleeve' model [40]. (a) A cartoon depicting a sleeve — a narrow cylinder capable of biased diffusion and connected to the dynamic end of the microtubule. (b) Free energy profile for the motion of an individual sleeve protein along the microtubule. Since the microtubule contains 13 protofilaments, the distance between the binding sites of the sleeve proteins and the microtubule is 8 nm/13 = 0.6 nm. In Hill's rigid structure, the energy barrier b for the transition of a microtubule-bound kinetochore protein from one binding site to another is lower in magnitude than the energy w required for the complete detachment of the protein from the microtubule at its end. (c) The sleeve wanders along the surface of the microtubule, synchronously moving all its binding elements. Greater overlap between the sleeve and the microtubule corresponds to lower free energy but requires more energy for the transitions. The figure is adapted from [40].

interact with 65 dimers. The inner part of Hill sleeve was supposed to be covered with microtubulebinding proteins; in the published model, the number of such proteins was also 65. Moreover, Hill indicated that the distance between adjacent sites for coupling with tubulin should be 6.15 Å. From this followed that either each tubulin dimer or the sleeve protein had 13 binding sites along its length. This assumption seems rather speculative. A key feature of Hill sleeve proteins is that they allow the sleeve to diffuse unidimensionally along the surface of the microtubule meaning that the sleeve proteins can jump from one binding site on the microtubule surface to another without losing their connection to the microtubule. In Hill's model, the assumption of surface diffusion without detachment is a natural consequence of the sleeve design, since the position of each protein is fixed in the rigid framework of the sleeve. This feature of the model has a pronounced effect on the interaction energy between the sleeve and the microtubule. The sleeve structure effectively reduces the energy barriers for the detachment of individual binding sites of the sleeve during its diffusion (parameter b, Fig. 8b, c) compared to the energy barrier that the sleeve must overcome to fully detach from tubulin at the end of the microtubule (parameter w). Moreover, each binding site of the sleeve can move only synchronously with the other 64 binding proteins in the sleeve — a specific and unique characteristic of such sleeve design. This ensemble of proteins, when brought into contact with the end of a microtubule, moves together with the sleeve as a whole, demonstrating biased diffusion toward a position that provides greater overlap with the microtubule surface. A deeper penetration of the microtubule into the sleeve corresponds to a greater number of bonds between the sleeve proteins and tubulin, and consequently, to a lower free energy of interaction between the coupler and the microtubule. The molecular 'roughness' of the interaction between the sleeve proteins and the microtubule, expressed by the parameter b, prevents the complete penetration of the microtubule into the sleeve, and they reach a dynamic stationary state at a certain depth. It is easy to see that if the end of the microtubule, inserted into this sleeve, begins to shorten, it causes a diffusive shift of the sleeve towards a new equilibrium position. The sleeve and the chromosome attached to it follow the shortening end of the microtubule, attempting to restore the overlap with reduced binding energy [42]. Using a known chromosome speed (around 1 μm min^{-1}), the chromosome's diffusion coefficient, and the geometric parameters of the sleeve, Hill determined the sleeve-microtubule interaction parameters to be $b = 0.3\,k_\text{B}T$ and $w = 2.5\,k_\text{B}T$. Under these conditions, the sleeve can withstand a relatively wide range of loads while moving at a constant speed. The latter feature resonates with the force-velocity dependency, as measured for chromosomes in grasshopper spermatocytes, where the velocity began to decline only at very high loads (about 100 pN; the load on a single microtubule is, of course, lower, since kinetochores bind many microtubules) [32]. However, in Hill model, the overlap between the sleeve and the microtubule decreases with increasing load until the sleeve finally detaches at 9 to 15 pN force per microtubule [42]. Thus, the sleeve is not very efficient in converting the energy released during the depolymerization of the microtubule: the efficiency is about 20–25%, which is consistent with more general estimates of the efficiency of biased diffusion.

Despite the fact that 40 years have passed since the publication of the work on Hill sleeve, there is still considerable interest in the sleeve model for chromosome entanglement. Nevertheless, subsequent discoveries have rendered unlikely the hypothesis that a mechanism similar to Hill's sleeve — or any other biased-diffusion device — operates in this system. One such discovery is a structural feature found at the end of depolymerizing and polymerizing microtubules, in the form of a crown of splaying, curved protofilaments [43–46]. The sleeve does not fit well with this geometry. At the time of Hill's publication, this fact was unknown. The second discovery revealed that heterodimeric Dam1 proteins are capable of forming rings around microtubules [47, 48]. At first, it seemed that a structure, in some way resembling a sleeve, had finally been found. However, further studies of this complex showed that the mechanism of the ring's motion is in no way a mechanism of biased diffusion. Most likely, another mechanism is present here — the 'power stroke' of the protofilament, which actively displaces the ring-shaped coupler as the microtubule depolymerizes. Let's take a closer look at this coupler protein.

3.2 Dam1 ring coupler

The ring coupler was theoretically proposed by Koshland et al. [49] in 1988, based on their discovery that shortening *in vitro* microtubules could maintain attachment to kinetochores on immobilized chromosomes, as well as on earlier descriptions of ring-shaped and helical tubulin oligomers that form under certain conditions of microtubule depolymerization [50]. The first theoretical analysis of force transmission by a flat, rigid ring that does not bind to the microtubule wall was carried out following the development of a quantitative molecular-mechanical model of the microtubule [35]. It was shown that the mechanism of a power stroke exerted on the ring by a bending protofilament as it detaches from the microtubule can provide maximal utilization of the deformation energy stored in the microtubule lattice and, consequently, can generate the maximum possible force, assuming that the ring coupler does not restrict complete dissociation of the lateral bonds

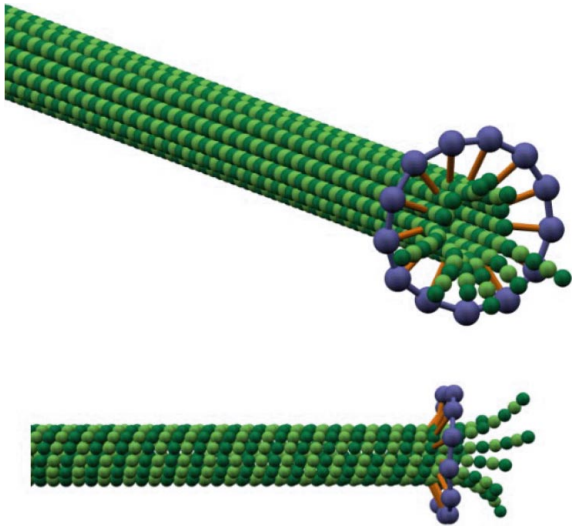

Figure 9. Dam1 ring coupler on a microtubule. Subunits of the Dam1 protein complex are shown as lilac spheres; the protrusions (linkers) mediating attachment to the microtubule are shown in orange.

between tubulin dimers. This means that the ring should not have an excessively small inner diameter; its optimal value is 35–40 nm for a microtubule diameter of 25 nm. For this reason, the power-stroke mechanism cannot operate within the narrow sleeve postulated by Hill [40]. Studies of ring structures received a major impetus when the first kinetochore complex with a ring geometry was discovered. Two teams — the Barnes/Drubin laboratory and the Harrison laboratory — found that a multisubunit complex from budding yeast, called Dam1 (or DASH), spontaneously assembles into rings of 15–16 subunits around the microtubule [47, 48]. The electron-dense core of the Dam1 ring is separated from the outer microtubule wall by a gap of 3–6 nm, a distance very similar to the 4–5 nm gap predicted for an energy-efficient ring coupling [35]. However, the typical distance for protein-protein interactions is much shorter than the gap between the core of the Dam1 ring and the microtubule wall. Based on these observations, it was proposed in [35] that the large diameter serves to maximize the energetic efficiency of the Dam1 ring, whereas adhesion to the microtubule wall is provided by radial linkers (Fig. 9) that are poorly visualized in structural data.

The theory developed on this basis emphasizes that the optimal performance of such a coupler will be achieved if the linkers are flexible, since rigid attachments effectively reduce the diameter of the ring. This prediction has not yet been tested directly, although structural studies suggest that the inward-pointing protrusions of the Dam1 ring are not rigid [51]. Moreover, the model prediction that such linkers should favor certain preferred orientations of the Dam1 ring on the microtubule wall was confirmed experimentally [37]. It is worth emphasizing that the flexibility of the linkers allows them to behave somewhat independently, in contrast to the Hill sleeve, in which all attachments between the microtubule and the sleeve dissociate and rebind synchronously.

3.3 Physical constraints on processive coupling by a Dam1-like ring

Just as the Hill sleeve was an embodiment of biased-diffusion mechanisms, the Dam1 ring has generally been discussed in connection with protofilament power strokes. However, modeling shows that the mechanism of motion of any ring is determined not so much by its geometry as by the parameters describing the binding of the ring to the microtubule. Depending on the strength of these interactions, the ring can move either by biased diffusion or by forced walking, and indeed even by a combination of these mechanisms [52].

If the energy with which each radial linker binds to the microtubule wall is relatively low ($0.5\,k_BT$), a ring with 13 such attachments will exhibit one-dimensional diffusion along the microtubule wall. When the microtubule depolymerizes, the splaying protofilaments can act as a barrier because their radial extent is considerably greater than the diameter of the ring. In this case, the thermal motion of the ring becomes biased. Although, technically, these bending protofilaments push the weakly bound ring when they come into contact with it, in the absence of load this aspect of their interaction is mechanically insignificant because of the low resistance of the ring to sliding. This scenario appears to provide a good explanation for how the ring can maintain processive coupling of chromosomes to a depolymerizing microtubule. However, as with other biased-diffusion mechanisms, the 'Achilles' heel' of such a process lies in its behavior under load. First, thermal fluctuations cannot sustain the transport of large cargoes at the end of a polymer shortening at physiologically relevant rates. Second, a weakly bound ring is unlikely to maintain stable attachment to the shortening microtubule end. For example, a binding energy of $3\,k_BT$ per spoke cannot prevent detachment of a ring forming 13 attachments to the microtubule wall when the load exceeds 6 pN [52].

The authors of [52] conclude that such a mechanism of ring coupling is theoretically possible and may provide an acceptable solution for microtubule-dependent transport in some biological systems in which slow movement kinetics and/or large loads are not a concern. However, a weakly bound ring cannot maintain its attachment to the microtubule end under large and variable loads. During mitosis, the kinetochore may occasionally experience a large load; a variable load or some stochastic event may stall depolymerization or trigger a switch to growth. The weaker the coupling of the ring to the microtubule wall, the more readily it detaches. Greater stability of ring attachment is achieved when the protrusions bind more strongly to the microtubule wall. However, if the binding is excessively strong, even powerful protofilament power strokes will no longer be able to move the ring along the microtubule wall, and the ring will block depolymerization. This consideration illustrates the dichotomy of the ring coupler arising from the antagonistic requirements for coupler attachment stability (higher binding energy) and coupler sliding (lower binding energy). The theory helps identify a range of ring affinities that provides an acceptable compromise — from 10 to $14\,k_BT$ per attachment [52]. For example, at $13\,k_BT$, the detachment force is predicted to increase to 40 pN, while such a ring can still be moved by the force generated by protofilament bending. It will exhibit no detectable diffusive motion and will therefore move exclusively with the microtubule end. In this case, each protrusion moves along a single protofilament, hopping from one binding site to another, much like an ATP-dependent motor protein such as kinesin, except that the energy driving ring movement is supplied by hydrolysis of GTP bound to tubulin.

3.4 Experimental analysis of Dam1-dependent coupling

Theoretical modeling revealed a relationship between the strength of the ring-microtubule coupling, the diffusion rate of the ring, and the extent to which an unloaded ring should slow the rate of microtubule depolymerization [52]. All these and other Dam1-dependent phenomena reflect different aspects of the interaction between Dam1 heterodecamers and the microtubule wall, and therefore their quantitative characteristics should be mutually consistent. However, the complexity of this system and the substantial discrepancies among published experimental measurements have led to conflicting views on the coupling mechanism of the actual Dam1 ring. The two most important parameters of the Dam1-tubulin interaction — their binding energy and the rate of Dam1 diffusion on the microtubule surface — are still under debate.

Westermann et al. [47] used a biochemical approach to estimate the dissociation constant between the Dam1 heterodecamer and the microtubule; their data suggest that this value lies in the submicromolar range. However, without knowledge of the Dam1 oligomerization pathway and the details of its binding to the microtubule, this constant does not uniquely determine the tubulin-Dam1 binding energy. Part of the observed binding energy could result from interactions among the components of the Dam1 complex themselves, so this value can only be used as an upper estimate for Dam1-microtubule binding ($\sim 1\,k_{\rm B}T$). However, the microtubule affinity of a mutant Dam1 complex with a reduced ability to form rings is similar to that of wild-type Dam1 [47, 53], suggesting that most of the observed interaction corresponds to Dam1-microtubule binding. Gestaut et al. [54], using a microscopy-based assay, concluded that the Dam1-microtubule affinity is two orders of magnitude stronger. However, it can be shown that GTP hydrolysis cannot provide sufficient energy to move a ring with such strong binding. The most straightforward measure of the interaction between a Dam1 ring encircling a microtubule can be obtained by analyzing the *in vitro* velocity of unloaded ring movement [55]. The observed velocity at which a Dam1 ring tracks a shortening microtubule implies a binding energy of 13–15 $k_{\rm B}T$ per Dam1-tubulin bond, consistent with the biochemical data [47].

As noted above, a ring with such moderately strong bonds should exhibit no observable diffusion on a biologically relevant timescale of many minutes. However, the first publication of this kind concluded that Dam1 rings diffuse very rapidly (0.05 $\mu m^2\ s^{-1}$) [56], although this interpretation did not take into account the ability of Dam1 heterodecamers to form different oligomeric complexes that vary in size and geometry [55]. Subsequent quantitative studies of Dam1 complex diffusion showed that this high diffusion coefficient characterizes the thermal motion of only one or two Dam1 subunits [54, 55]; larger Dam1 oligomers diffuse much more slowly [55]. These observations place the diffusion coefficient of a complete Dam1 ring at $10^{-7}\ \mu m^2\ s^{-1}$, implying a Dam1-tubulin binding energy of more than 7 $k_{\rm B}T$.

3.5 Fibrillar protein complexes as couplers in mammalian cells

Despite compelling evidence that the Dam1 complex can act as a coupler linking chromosome movement to microtubules in yeast, no homologs or even analogous complexes capable of forming rings around microtubules have been identified in higher organisms such as mammals [57, 58].

Electron tomography of mammalian kinetochores, however, revealed thin fibrils connecting curved protofilaments directly to the inner region of the kinetochore. A quantitative analysis of the shape of microtubule ends attached to kinetochores showed that the protofilaments of these microtubules have a different shape from those at the ends of microtubules growing or shortening *in vitro* [58]. The association of protofilaments with fibrils correlates with their local straightening, suggesting that these conformational changes are caused by forces acting through the fibrils.

These experimental findings inspired the authors of [58] to develop a computer model of a fibril-based coupler. Using the previously developed molecular-mechanical model of depolymerizing microtubules and introducing kinetochore fibrils as springs connecting tubulin in the bending protofilaments to the chromosome, it was possible to analyze a theoretical design of a new type of coupler (Fig. 10).

In the model considered, fibrils were assumed to be present in unlimited numbers and to bind tubulin at random sites along the protofilaments, but not to bind soluble tubulin. As the protofilaments tend toward their minimum-energy conformation, they exert a power stroke on the bound fibril, thereby driving chromosome movement. When tubulin depolymerizes from the tip of a bending protofilament, the bound fibril is released and returns to the pool of fibrils interacting with the protofilaments.

Under these assumptions, the model demonstrated that protofilament power strokes can steadily move a cargo against a substantial load. The analysis showed that such a hypothetical coupler would be even more energy-efficient than the Dam1 ring. A ring that binds microtubules strongly enough to ensure processive coupling, impedes microtubule shortening and reduces the useful work that can be performed by microtubule

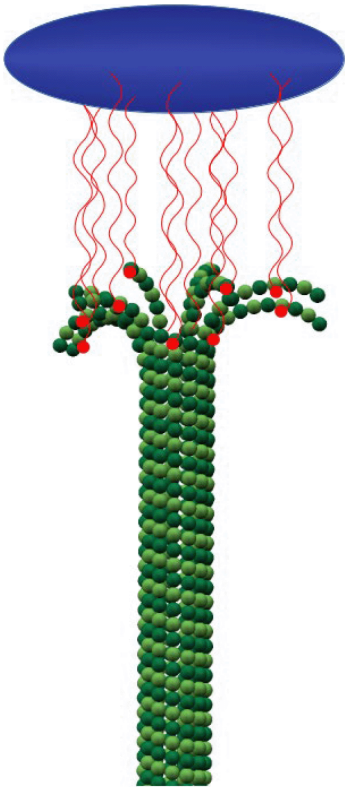

Figure 10. Model of the fibrillar coupler proposed in [58]. Fibrillar proteins connecting the microtubule end to the chromosome are shown in red.

depolymerization [37]. In contrast, a fibrillar coupler does not need to move from one binding site to another along the microtubule wall; the fibrils undergo cycles of detachment and reattachment, and therefore the efficiency of the depolymerization motor is not limited. This feature may be particularly valuable in cells in which chromosomes are large or experience substantial forces opposing their movement.

However, fibrils have an obvious disadvantage: they bind to microtubule protofilaments stochastically and independently of one another. Thus, if some of them fail to form strong attachments, unbound protofilaments may lose their connection to the chromosome. In a real microtubule, the appearance of freely detaching protofilaments would most likely lead to microtubule disassembly, and the connection to the chromosome would be lost. This fibril-based model is far from providing satisfactory answers to all physiological questions concerning the coupling of microtubule depolymerization to the kinetochore. For example, it does not explain how chromosomes can move at the ends of elongating microtubules. Rather, this model should be regarded as a prototype of a new coupling strategy driven by a power-stroke-dependent mechanism, which does not rely on a rigid encircling structure but is capable of operating without sliding along the microtubule wall.

Various proteins with an appropriately elongated structure have been considered for the role of a fibrillar coupler, such as CENP-F [59], CENP-E [60, 61], and the kinetochore Ndc80 complex [62]. Most current work is focused specifically on the latter — the multisubunit Ndc80 complex, which has been found in the kinetochores of all eukaryotes studied to date [63]. It is a highly elongated protein complex (about 60 nm) [64], without which the kinetochore almost does not bind to the microtubule end.

Individual molecules of the Ndc80 complex are unable to processively track the ends of assembling and disassembling microtubules. However, they acquire this ability when organized into clusters [65, 66]. Interestingly, in yeast cells, it is the Ndc80 complex that acts as a kind of suspension system for the Dam1 complex, through which the ring coupler is attached to the chromosome [67]. *In vitro* experiments have shown that the interaction of Dam1 with Ndc80 enables Ndc80 to track the ends of growing and shortening microtubules, indicating that these complexes work effectively in tandem [68, 69].

A very recent study of the interaction of individual Ndc80 complex molecules with microtubules using ultrafast force spectroscopy revealed a remarkable ability of this protein to move along the microtubule surface with a resistance that varies greatly depending on the direction of movement and the applied force [70]. When the force is directed so as to pull the molecule off the microtubule plus end, i.e., away from the chromosome, the resistance increases sharply and rises rapidly with increasing force. The binding strength of a single Ndc80 molecule to the microtubule gradually increases from $6-7\,k_BT$ to $12-13\,k_BT$. We remind the reader that stabilization of velocity over a broad range of forces had previously been documented in the classic experiments on grasshopper spermatocytes, in which the velocity of chromosomes moving with the ends of depolymerizing microtubules began to decrease only under substantial opposing loads [32]. Thus, the ability of the Ndc80 complex to change its resistance depending on the applied force provides an additional strong argument in favor of the fibrillar coupler, but also points to a more complex organization of this coupler than previously thought.

4. Conclusion

Studies over the past two decades have shown that microtubules are not only used by the cell as static structural elements of the cytoskeleton. Depolymerizing microtubules are capable of generating forces that are very significant on the cellular scale. These forces arise from the unique mechanochemical features of tubulin polymerization. Each microtubule is like a loaded spring: GTP bound to tubulin is hydrolyzed, and a significant part of the chemical energy released in this process is stored as strained conformational deformation in the microtubule wall and is released when tubulin bends during its depolymerization. Linear tubulin filaments, called 'protofilaments,' bend as they depolymerize, allowing them to work as motors. Theory predicts that the resulting force developed in such a mechanochemical process can be large.

The ability of proteins to change their conformation as a result of biochemical reactions is apparently one of the most ancient properties of proteins. The simplest change consisting in a slight bending of the tubulin molecule leads to the generation of significant forces due to the linear organization of protofilaments capable of bending. Perhaps, Nature used these forces primarily for chromosome movement in eukaryotic cells, because before inventing a way to mechanically separate sister copies of DNA in space, the process of cellular self-reproduction could not have arisen. In essence, without this essential evolutionary step, the process of cell reproduction was impossible. And without cell reproduction, there is no life and no evolution of living organisms. In the course of further evolution, other, diverse and in some respects more efficient molecular motors appeared, which perform a variety of mechanical tasks in our body. But the process of chromosome segregation (mitosis) continues to use this primitive and apparently most ancient motor. In no cell type or organism has Nature replaced it with a more advanced one. Apparently, all evolutionary attempts to change this mechanism inevitably led to disruption of cell division and, consequently, to elimination from evolution.

The question of the organization of couplers — protein complexes at the kinetochore that couple the mechanical movements of protofilaments during microtubule depolymerization to chromosome movement — remains open and of primary importance. They ensure stable attachment of the chromosome to the depolymerizing microtubule end even in the presence of large opposing forces and despite the stochastic nature of tubulin dynamics. Several coupler designs — one based on the Hill sleeve, another on a ring, and a third on elongated fibrils — have now been reasonably well studied theoretically, making it possible to compare their characteristic features, such as energy-transfer efficiency, attachment stability, and the force–velocity relationship. The ring coupler has been particularly well studied; the discovery of the multiprotein Dam1 ring made it possible to carry out an in-depth analysis of its design and function. The biomechanical properties of the yeast Dam1 ring, such as its large diameter, flexible linkers, and relatively strong binding, appear to be finely tuned to allow this coupler to move under load without detaching. However, Nature has abandoned this elegant device in all cell types in the vast majority of multicellular organisms — apparently in favor of a more efficient coupler, most likely a fibrillar one. Active research in this field continues, and there is a reason to hope that the near future will bring progress comparable to that seen in recent years in understanding the mechanisms of the ring coupler operation.

Acknowledgments. The authors are grateful to Prof. E.L. Grishchuk and Prof. J.R. McIntosh for numerous helpful discussions. This work was supported by the Russian Science Foundation, grant No. 25-74-20038 https://rscf.ru/project/25-74-20038/.

References

1. Blumenfeld L A *Reshaemye i Nereshaemye Problemy Biologicheskoi Fiziki* (Solvable and Unsolvable Problems of Biological Physics) (Moscow: URSS, 2002)
2. Reck-Peterson S L et al. *Nature Rev. Mol. Cell Biol.* **19** 382 (2018)
3. Yildiz A *Nature Rev. Mol. Cell Biol.* **26** 86 (2025)
4. Titus M A *Cold Spring Harb. Perspect. Biol.* **10** (3) a021972 (2018) DOI:10.1101/cshperspect.a021972
5. Clapier C R et al. *Nature Rev. Mol. Cell Biol.* **18** 407 (2017)
6. Bourgeois C F, Mortreux F, Auboeuf D *Nature Rev. Mol. Cell Biol.* **17** 426 (2016)
7. Murrell M et al. *Nature Rev. Mol. Cell Biol.* **16** 486 (2015)
8. Sweeney H L, Holzbaur E L F *Cold Spring Harb. Perspect. Biol.* **10** (5) a021931 (2018) DOI:10.1101/cshperspect.a021931
9. Romanovsky Yu M, Tikhonov A N *Phys. Usp.* **53** 893 (2010); *Usp. Fiz. Nauk* **180** 931 (2010)
10. Zakharov P N et al. *Phys. Usp.* **59** 773 (2016); *Usp. Fiz. Nauk* **186** 853 (2016)
11. Alberts B et al. *Molecular Biology of the Cell* 7th ed., Intern. Student Ed. (New York: W.W. Norton and Co., 2022)
12. Gudimchuk N B, McIntosh J R *Nature Rev. Mol. Cell Biol.* **22** 777 (2021)
13. Gard D L, Kirschner M W *J. Cell Biol.* **105** 2203 (1987)
14. Traut T W *Mol. Cell. Biochem.* **140** (1) 1 (1994)
15. Romani A, Scarpa A *Arch. Biochem. Biophys.* **298** (1) 1 (1992)
16. Desai A, Mitchison T J *Annu. Rev. Cell Dev. Biol.* **13** (1) 83 (1997)
17. Gudimchuk N B, Alexandrova V V *Biophys. Rev.* **15** 1095 (2023)
18. Nogales E et al. *Nature Struct. Biol.* **5** 451 (1998)
19. Beckett D, Voth G A *Proc. Natl. Acad. Sci. USA* **120** e2305899120 (2023) DOI:10.1073/pnas.2305899120
20. Carlier M F, Pantaloni D *Biochemistry* **20** 1918 (1981)
21. Maccioni R, Seeds N W *Proc. Natl. Acad. Sci. USA* **74** 462 (1977) DOI:10.1073/pnas.74.2.462
22. Mitchison T, Kirschner M *Nature* **312** 237 (1984)
23. Nogales E *Annu. Rev. Biophys. Biomol. Struct.* **30** 397 (2001)
24. Mandelkow E M, Mandelkow E, Milligan R A *J. Cell Biol.* **114** 977 (1991)
25. Duellberg C et al. *eLife* **5** e13470 (2016)
26. Hyman A A et al. *Mol. Biol. Cell.* **3** 1155 (1992)
27. Bowne-Anderson H et al. *BioEssays* **35** 452 (2013)
28. Gardner M K et al. *Cell* **147** 1092 (2011)
29. Coombes C E et al. *Curr. Biol.* **23** 1342 (2013)
30. Alexandrova V V et al. *Proc. Natl. Acad. Sci. USA* **119** e2208294119 (2022) DOI:10.1073/pnas.2208294119
31. Farmer V J, Zanic M *BioEssays* **45** 2200081 (2023)
32. Nicklas R B *J. Cell. Biol.* **97** 542 (1983)
33. Grishchuk E L et al. *Nature* **438** 384 (2005)
34. Grishchuk E L, Ataullakhanov F I *Meth. Cell. Biol.* **95** 657 (2010)
35. Molodtsov M I et al. *Proc. Natl. Acad. Sci. USA* **102** 4353 (2005)
36. Grishchuk E L et al., in *Comprehensive Biophysics* Vol. 4 (Ed. E Egelman) (New York: Elsevier, 2012) pp. 93–117, DOI:10.1016/B978-0-12-374920-8.00409-4
37. Grishchuk E L et al. *Proc. Natl. Acad. Sci. USA* **105** 15423 (2008)
38. O'Brien E T et al. *Biochemistry* **29** 6648 (1990)
39. Rieder C L, Salmon E D *Trends Cell Biol.* **8** (8) 310 (1998)
40. Hill T L *Proc. Natl. Acad. Sci. USA* **82** 4404 (1985)
41. Wollman R et al. *Curr. Biol.* **15** 828 (2005)
42. Joglekar A P, Hunt A J *Biophys. J.* **83** (1) 42 (2002)
43. Höög J L et al. *J. Cell Sci.* **124** 693 (2011) DOI:10.1242/jcs.072967
44. McIntosh J R et al. *J. Cell Biol.* **217** 2691 (2018)
45. Gudimchuk N B et al. *Nature Commun.* **11** 3765 (2020) DOI:10.1038/s41467-020-17553-2
46. Iyer S S et al. *J. Cell Biol.* **224** e202406061 (2025)
47. Westermann S et al. *Mol. Cell* **17** (2) 277 (2005)
48. Miranda J L et al. *Nature Struct. Mol. Biol.* **12** (2) 138 (2005)
49. Koshland D E, Mitchison T J, Kirschner M W *Nature* **331** 499 (1988)
50. Kirschner M W, Honig L S, Williams R C *J. Mol. Biol.* **99** 263 (1975) DOI:10.1016/S0022-2836(75)80144-6
51. Miranda J L, King D S, Harrison S C *Mol. Biol. Cell* **18** 2503 (2007)
52. Efremov A el al. *Proc. Natl. Acad. Sci. USA* **104** 19017 (2007)
53. Wang H-W et al. *Nature Struct. Mol. Biol.* **14** 721 (2007)
54. Gestaut D R et al. *Nature Cell Biol.* **10** 407 (2008)
55. Grishchuk E L et al. *Proc. Natl. Acad. Sci. USA* **105** 6918 (2008)
56. Westermann S et al. *Nature* **440** 565 (2006)
57. McIntosh J R et al. *J. Cell Biol.* **200** 459 (2013)
58. McIntosh J R et al. *Cell* **135** (2) 322 (2008)
59. Volkov V A et al. *J. Cell Biol.* **209** 813 (2015)
60. Putkey F R et al. *Developmental Cell* **3** 351 (2002)
61. Gudimchuk N et al. *Nature Cell Biol.* **15** 1079 (2013)
62. Ustinov N B, Korshunova A V, Gudimchuk N B *Biochemistry Moscow* **85** 448 (2020) DOI:10.1134/S0006297920040057
63. Wei R R, Sorger P K, Harrison S C *Proc. Natl. Acad. Sci. USA* **102** 5363 (2005)
64. Welburn J P I, Cheeseman I M *Developmental Cell* **15** 645 (2008)
65. Powers A F et al. *Cell* **136** 865 (2009) DOI:10.1016/j.cell.2008.12.045
66. Volkov V A et al. *eLife* **7** e36764 (2018) DOI:10.7554/eLife.36764
67. Jenni S, Harrison S C *Science* **360** 552 (2018)
68. Tien J F et al. *J. Cell Biol.* **189** 713 (2010)
69. Lampert F, Hornung P, Westermann S *J. Cell Biol.* **189** 641 (2010)
70. Demidov V M et al. *Sci. Adv.* **11** eadx0005 (2025)